

## HIGH DAMPING RUBBER BEARING ISOLATORS: QUASI- LINEAR MECHANICAL MODEL FORMULATIONS

Athanasios A. Markou<sup>1</sup>, and George D. Manolis<sup>2</sup>

<sup>1</sup>Norwegian Geotechnical Institute  
Oslo N-0855, Norway  
e-mail: [athanasiosmarkou@gmail.com](mailto:athanasiosmarkou@gmail.com)

<sup>2</sup>Department of Civil Engineering, Aristotle University  
Thessaloniki GR-54124, Greece  
e-mail: [gdm@civil.auth.gr](mailto:gdm@civil.auth.gr)

**Keywords:** High Damping Rubber Bearings; Mechanical Models; Loading and Unloading Cycles; Nonlinear Response; Base Isolation.

**Abstract.** *In this work, we present two sub-categories of models for reproducing the mechanical response of high damping rubber bearings, which is a base isolation system that is commonly used for buildings in seismically-prone regions of the EU. These are the trilinear models that have evolved from the more standard group of bilinear models. These trilinear models are built by combining linear and nonlinear elastic springs, as well as sliders, while the connectivity of these elements can be either in series or in parallel, which yields the two basic sub-categories of first type and second types. The best fit with experimentally obtained results involving time-harmonic tests on a commercial high damping base isolator at shear amplitudes up to 200% is achieved by the trilinear hysteretic system of the first type. Future extensions to bi-directional horizontal motion and to time-varying vertical loads is currently under consideration.*

## 1 INTRODUCTION

High damping rubber bearings (HDRB) have been used for seismic isolation of structures worldwide since the 1980's. Given the highly nonlinear material behavior of these devices, no single mathematical model can capture every aspect of their dynamic response [1]. Issues and uncertainties involved in the characterization of their mechanical behavior are coupled bidirectional horizontal motion, coupling of vertical and horizontal motion, strength and stiffness degradation during cyclic loading, and variation in critical buckling load capacity due to lateral displacements. Elementary mechanical models for base isolators comprise (a) a spring to model the elastic response, (b) a plastic slider for time-independent plasticity and (c) a dashpot for viscosity [2]. The simplest model to describe the time-independent plasticity is the bilinear hysteretic model (BHM), which has been used for decades now and combines springs with a plastic slider. In addition to the BHM, smooth hysteretic models have been developed [3]. Furthermore, there exist two basic BHM sub-formulations [1,4]. However, materials like high damping rubber bearings (HDRB) exhibit hardening behavior at large strain amplitudes. In order to account for this effect, an extension of the BHM was developed as the trilinear hysteretic model (THM) [5,6]. Apart from use for the simulation of the shear behavior of HDRB, the THM has been used also for single, double and triple friction pendulums, as well as for partition anti-seismic wall elements [7,8]. The present work investigates two possible variations of the THM that account for either hardening or softening behavior and highlights their differences. To this end, a set of cyclic shear tests on a spare HDRB specimen from the Solarino, Italy building base isolation project [9] are used to validate and subsequently compare these models in terms of their accuracy.

## 2 MECHANICAL FORMULATION FOR QUASI-LINEAR HYSTERETIC MODEL

As an extension of BHM to THM, we have the THM1 and THM2 variations in Figs. 1 and 2, respectively [1,6]. More specifically, the parent element BHM1 of THM1 that consists of a linear elastic spring of stiffness  $k_e^{m1}$  (element 1) connected in series with a parallel system, i.e., a plastic slider with characteristic force  $f_s^{m1}$  (element 2) and a linear elastic spring of stiffness  $k_{h1}^{m1}$  (element 3), is modified by replacing element 3 with a trilinear elastic spring. The parameters now needed to describe this trilinear elastic spring (element 3) are the stiffnesses  $k_{h1}^{m1}, k_{h2}^{m1}$  and the characteristic displacement  $u_c^{m1}$ . A positive displacement  $u_c^{m1}$  denotes change of slope in the spring from  $k_{h1}^{m1}$  to  $k_{h2}^{m1}$  and vice-versa for positive displacements  $u_h^{m1}$ , while a negative displacement  $-u_c^{m1}$  denotes the change of slope between  $k_{h1}^{m1}$  and  $k_{h2}^{m1}$ , for negative displacements  $u_h^{m1}$ . In the case of THM2, this new three-parameter trilinear spring (element 3) has stiffnesses  $k_{h1}^{m2}, k_{h2}^{m2}$  characteristic displacement  $u_c^{m2}$ . As in the previous case, a positive displacement  $u_c^{m2}$  denotes change of slope in the spring from  $k_{h1}^{m2}$  to  $k_{h2}^{m2}$  and vice-versa for positive displacements  $u$ , while a negative displacement  $-u_c^{m2}$  denotes the change of slope between  $k_{h1}^{m2}$  and  $k_{h2}^{m2}$  for negative displacements  $u$ . The relationships established between the parameters of the mathematical model  $(k_0, k_1, k_2, u_y, u_{yh})$  and those used for the corresponding mechanical  $(k_e, k_{h1}, k_{h2}, u_c, f_s)$  one are presented in Table 1 for both THM. Furthermore, the relationships between the mechanical parameters of the two systems are presented in Table 2, the compatibility equations are presented in Table 3, the equilibrium equations in Table 4 and finally the constitutive equations in Table 5. In the mathematical model, stiffness  $k_0$  corresponds to the elastic phases, stiffness  $k_1$  corresponds to plastic phase 2, and stiffness

| Model                   | THM1   | THM2                  |
|-------------------------|--|-----------------------|
| $k_e$                   | $k_0$  | $k_0$                 |
| $k_{h1}$                | $k_1 \frac{k_0}{k_0 - k_1}$                                  | $k_1$                 |
| $k_{h2}$                | $k_2 \frac{k_0}{k_0 - k_2}$                                  | $k_2$                 |
| $f_s$                   | $k_0 u_y = F_y$  | $(k_0 - k_1) u_y = Q$ |
| $u_c$                   | $(u_{yh} - u_y) \frac{k_0 - k_1}{k_0}$                       | $u_{yh}$              |
| $k_e - k_{h1} + k_{h2}$ | $k_0 \frac{k_0^2 - k_1(2k_0 - k_2)}{(k_0 - k_1)(k_0 - k_2)}$ | $k_{01}$              |

Table 1: Relationships between mechanical and mathematical parameters for THM

|      |            |   |   |  |  |
|------|------------|---|---|--|--|
| THM1 | $k_e^{m1}$ | $k_{h1}^{m1}$   | $k_{h2}^{m1}$   | $f_s^{m1}$   | $u_c^{m1}$   |
| THM2 | $k_e^{m2}$ | $k_{h1}^{m2} \frac{k_e^{m2}}{k_e^{m2} - k_{h1}^{m2}}$ | $k_{h2}^{m2} \frac{k_e^{m2}}{k_e^{m2} - k_{h2}^{m2}}$ | $f_s^{m2} \frac{k_e^{m2}}{k_e^{m2} - k_{h1}^{m2}}$ | $u_c^{m2} \frac{k_e^{m2} - k_{h1}^{m2}}{k_e^{m2}} - \frac{f_s^{m2}}{k_e^{m2}}$ |

Table 2: Relationships between the mechanical parameters of THM1 and THM2

| Model | THM1                  | THM2                  |
|-------|-----------------------|-----------------------|
| $u$   | $u_e^{m1} + u_h^{m1}$ | $u_e^{m2} + u_h^{m2}$ |

Table 3: Compatibility equations for the THM

| Model | THM1                       | THM2                                |
|-------|----------------------------|-------------------------------------|
| $f$   | $f_{e1} = f_{e2} + f_{e3}$ | $f_{e1} + f_{e3} = f_{e2} + f_{e3}$ |

Table 4: Equilibrium equations for the THM

| Model                       | THM1  | THM2  |
|-----------------------------|---|---|
| $f_{e1}$                    | $k_e^{m1} u_e^{m1}$   | $(k_e^{m2} - k_{h1}^{m2}) u_e^{m2}$                                   |
| $f_{e2} (\dot{u}_h \neq 0)$ | $f_s^{m1} \text{sgn}(\dot{u}_h^{m1})$   | $f_s^{m2} \text{sgn}(\dot{u}_h^{m2})$                                 |
| $f_{e2} (\dot{u}_h = 0)$    | $f_{e1} - f_{e3}$   | $f_{e1}$  |
| $f_{e3} ( u_h^*  \leq u_c)$ | $k_{h1}^{m1} u_h^{m1}$  | $k_{h1}^{m2} u$   |
| $f_{e3} ( u_h^*  > u_c)$    | $(k_{h1}^{m1} u_c^{m1} + k_{h2}^{m1} ( u_h^{m1}  - u_c^{m1})) \text{sgn}(u_h^{m1})$ | $(k_{h1}^{m2} u_c^{m2} + k_{h2}^{m2} ( u  - u_c^{m2})) \text{sgn}(u)$ |

Table 5: Constitutive equations for the THM

 \* For THM2 replace  $u_h^*$  with  $u$ 

| Model    | THM1  | THM2  |
|----------|---|---|
| $u_{ha}$ | $\frac{k_e^{m1} u_a - f_s^{m1} + u_c^{m1} (k_{h2}^{m1} - k_{h1}^{m1})}{k_e^{m1} + k_{h2}^{m1}}$ | $u_a - \frac{f_s^{m2}}{k_e^{m2} - k_{h1}^{m2}}$ |
| $W_d$    | $4 f_s^{m1} u_{ha}^{m1}$  | $4 f_s^{m2} u_{ha}^{m2}$                        |

 Table 6: Energy dissipation over a cycle of amplitude  $u_a$  for the THM1 and THM2

$k_2$  corresponds to plastic phases 1 and 3 (see Figs. 1 and 2). In the case of THM2, there is an additional additional elastic phase described by stiffness  $k_{01}$  (see Figs. 2(e)). The yield displacement is denoted as  $u_y$ , the second yield displacement is denoted as  $u_{yh}$ , the yield force at  $u_{yh}$  is denoted as  $F_{yh}$ , while the characteristic strength at zero displacement is denoted as  $Q$  and finally the yield force at  $u_y$  is denoted as  $F_y$ . The differences between these two sub-categories of models are as follows:

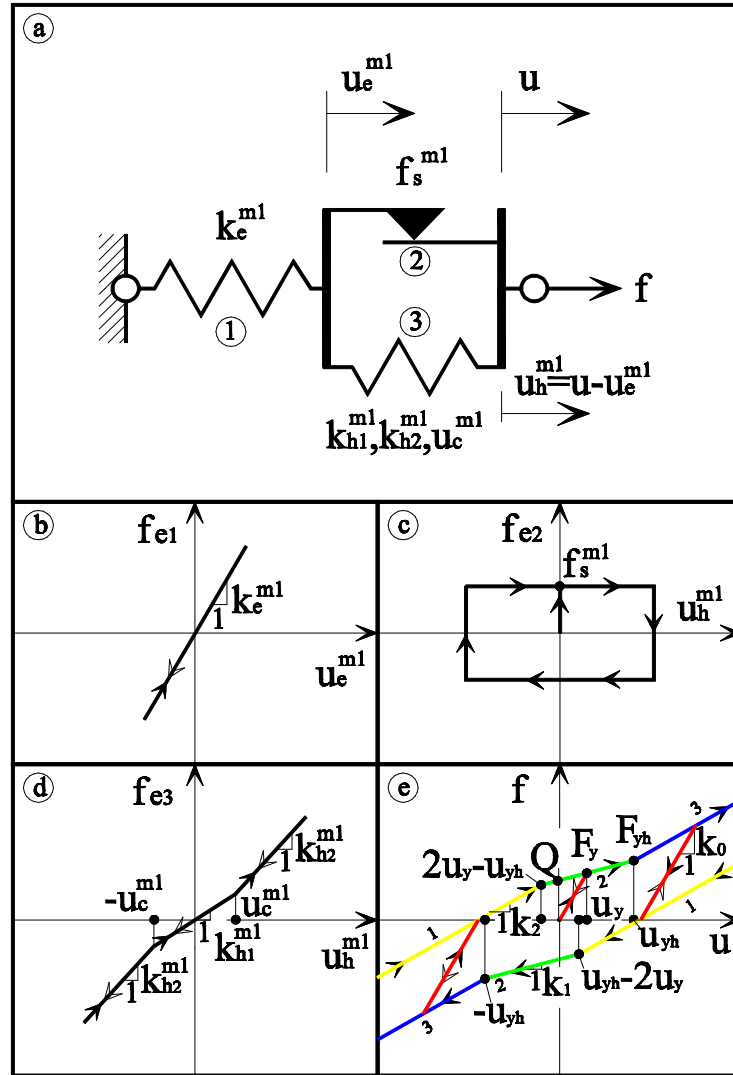


Figure 1: Trilinear hysteretic model labeled THM1

(a) THM1 exhibits three plastic phases (1,2,3) and one elastic phase with slope equal to  $k_0 = k_e^{m1}$ , see Fig. 1. On the other hand, THM2 also exhibits three plastic phases (1,2,3) and two elastic phases according to the displacement amplitude.

(b) The change of slope in the THM2 plastic phases occurs at displacement  $u_{yh}$  for  $u > 0$  and at  $-u_{yh}$  for  $u < 0$ . In THM1, the change of slope in the plastic phases occurs at displacement

$u_{yh}$  for  $u > 0$  and at  $-u_{yh}$  for  $u < 0$  during the loading ( $\dot{u}u > 0$ ), and at displacements  $u_{yh} - 2u_y$  for  $u > 0$  and at  $2u_y - u_{yh}$  for  $u < 0$  during the unloading phases ( $u\dot{u} < 0$ ).

(c) The dissipated energy over a cycle of amplitude  $u_a$  is denoted as  $W_d$  in both THMs and presented in Table 6, where  $u_{ha}$  denotes the displacement  $u_h$  at displacement amplitude equal to  $u_a$ . In order to have a dissipative system,  $u_{ha}$  and subsequently  $W_d$  need to be positive.

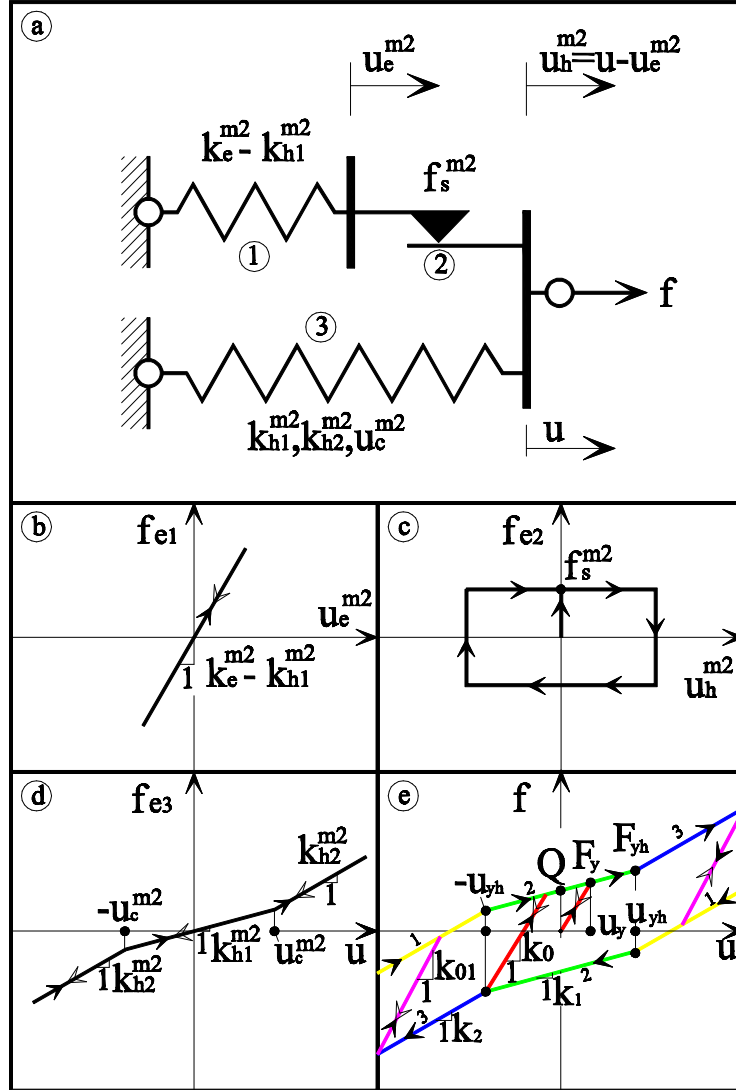


Figure 2: Trilinear hysteretic model labeled THM2

We assume that the energy dissipated in the THM1 is  $W_d^t$  at amplitude  $u_a$ , and is larger than the dissipated energy in the BHM1 ( $W_d^b$ ):

$$W_d^t > W_d^b \Leftrightarrow \frac{k_e^{m1} u_a - f_s^{m1} + u_c^{m1} (k_{h2}^{m1} - k_{h1}^{m1})}{k_e^{m1} + k_{h2}^{m1}} > \frac{k_e^{m1} u_a - f_s^{m1}}{k_e^{m1} + k_{h1}^{m1}} \quad (1)$$

Note that for the bilinear case  $k_{h1}^{m1} = k_{h2}^{m1}$  and  $u_{ha}^{m1} = \frac{k_e^{m1}u_a - f_s^{m1}}{k_e^{m1} + k_{h1}^{m1}}$ . For THM1 to account for larger dissipated energy than the BHM1, the following inequalities must be satisfied in terms of the mechanical and mathematical parameters, respectively:

$$(k_{h2}^{m1} - k_{h1}^{m1})(-k_e^{m1}(u_a - u_c^{m1}) + f_s^{m1} + k_{h1}^{m1}u_c^{m1}) > 0 \quad (2)$$

$$(k_1 - k_2)(u_a - u_{yh}) > 0 \quad (3)$$

For all THM  $u_a > u_{yh}$ , implying that term  $(u_a - u_{yh})$  is positive. For THM1 to account for larger energy dissipation as compared to BHM1, the inequality  $k_1 > k_2$  must also be satisfied. This last inequality shows that the THM1 can dissipate larger amounts of energy in comparison with the BHM1, but only for softening cases ( $k_1 > k_2$ ). In the case of hardening ( $k_1 < k_2$ ), the energy in THM1 decreases as compared to BHM1. This outcome can be explained physically, by realizing that the dissipation of all systems is related only to element 2, namely the plastic slider. As element 3 of THM1 becomes stiffer in the case of hardening, it allows for smaller displacements  $u_h$  in the plastic slider and therefore the dissipation of the system decreases. The opposite is true for the softening case.

It is also of interest to point out that each of the components of the THM2 is a particular case of the THM1 formulation. More specifically, THM1 can be simplified to a trilinear elastic spring for  $f_s^{m1} = 0$  and  $k_e^{m1} \gg k_{h1}^{m1}, k_{h2}^{m1}$  in terms of mechanical parameters, and in terms of mathematical ones with  $u_y = 0$  and  $k_0 \gg k_1, k_2$ , see Fig. 3(a). In this case, element 1 of THM1 will be extremely stiff to account for any deformation and will be neglected, while element 2 will not account for any dissipation ( $f_s^{m1} = 0$ ) and will also be neglected, so the system will behave linearly. The relation between mechanical and mathematical parameters (by taking into account that  $\frac{k_0}{k_0 - k_1} \simeq \frac{k_0}{k_0 - k_2} \simeq \frac{k_0 - k_1}{k_0} \simeq 1$ , see Table 1) is the following:  $k_{h1}^{m1} = k_1$ ,  $k_{h2}^{m1} = k_2$  and  $u_c^{m1} = u_{yh}$ , which results to a three-parameter system. Let us finally consider the stiffness of element 3 of the THM1 to be zero, namely  $k_{h1}^{m1} = k_{h2}^{m1} = 0$  and in mathematical terms  $k_1 = k_2 = 0$ , see Fig. 3(b). In this case, the THM1 will behave like any elastoplastic element and the relation between mechanical and mathematical parameters will be  $k_e^{m1} = k_0$  and  $f_s^{m1} = k_0 u_y$  (see Table 1), which results in a two-parameter system.

### 3 PARAMETER IDENTIFICATION USING HDRB CYCLIC SHEAR TESTS

In this section, the third cycle of a set of cyclic shear tests that were conducted on a commercial HDRB isolator from the Solarino project at the University of Basilicata in Italy [9] were used for the parameter identification using either THM1 or THM2. The geometrical characteristics of the HDRB are given in Table 7. The cyclic shear tests were conducted under

a compressive stress of  $6\text{ MPa}$  and at a frequency  $0.5\text{ Hz}$ , for ten different strain amplitudes varying from  $\gamma = 0.05$  to  $\gamma = 2$ . In parallel, cyclic tests at different strain amplitudes ( $\gamma = 1.20$  and  $\gamma = 2.00$ ) at variable frequencies (from  $0.006\text{ Hz}$  to  $0.83\text{ Hz}$ ) were implemented to investigate the effect of rate-dependence of the bearings. The tests showed that the HRDB isolator can be assumed rate-independent in this range of frequencies.

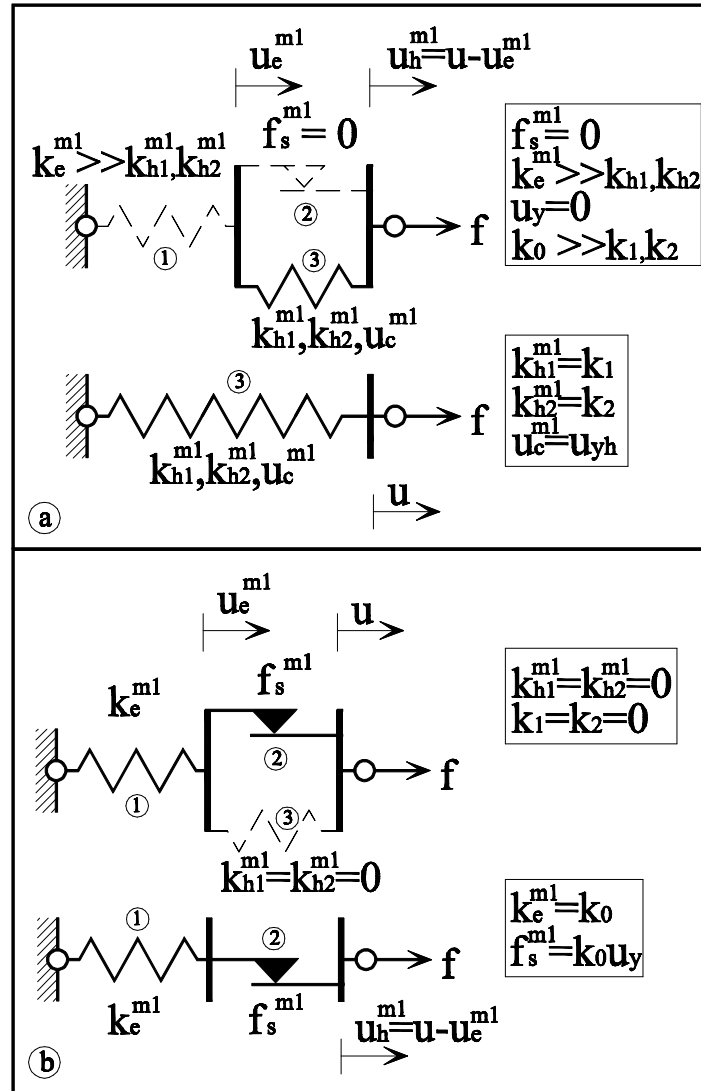


Figure 3: Simplifications of THM1: (a) a trilinear elastic spring and (b) an elastoplastic element

|   |           |
|---|-----------|
| External diameter (mm)                      | 500       |
| Diameter of steel plates $D$ (mm)           | 490       |
| Thickness of steel plates (mm)              | 3         |
| Number of rubber layers                     | 12        |
| Rubber layer thickness $T_r$ (mm)           | 8         |
| Total rubber thickness $T_r$ (mm)           | 96        |
| Cross section area $A_r$ (mm <sup>2</sup> ) | 188574.10 |
| Total height (mm)                           | 169       |
| Primary shape factor $S_1$                  | 15.31     |
| Secondary shape factor $S_2$                | 5.10      |

Table 7: Geometrical characteristics of the HDRB isolator

Next, two different rate-independent parallel models are used to describe the cyclic shear tests, one being the THM1 and the other THM2. The identification procedure that was used for the definition of the parameters is the CMA-ES algorithm [10]. In Table 8, the identified mathematical parameters of the THM1 system are presented along with the corresponding mechanical formulations. The identification error  $e^2$  is defined as follows:

$$e^2 = \sum_{i=1}^{10} \frac{\langle F_{0i} - \tilde{F}_i, F_{0i} - \tilde{F}_i \rangle}{\langle F_{0i}, F_{0i} \rangle} \quad (4)$$

where  $F_{0i}$  and  $\tilde{F}_i$  are the measured and computed force vectors at ten different strain amplitudes, and  $\langle A, B \rangle$  is the inner vector product. Nine THM1 components are connected in parallel to describe the shear behavior of the HRDB, but some of them represent simplified versions of THM1, see Fig. 3. Specifically, we have the trilinear elastic spring (components 1, 2 and 3) and the elastoplastic element (components 8 and 9).

We note that the trilinear elastic springs (components 1, 2 and 3) are hardening springs ( $k_2 > k_1$ ) accounting for the hardening behavior of the device at higher strain amplitudes, see Fig. 4(a). On the other hand, components 4, 5, 6 and 7 give softening behavior ( $k_2 < k_1$ ), while in all of these cases  $k_2$  is negative, see Figs. 4(b-e). These four components are responsible for describing the increase of dissipated energy as the strain amplitude increases. This combination provides a better description of the behavior during the loading ( $u\dot{u} > 0$ ) and unloading ( $u\dot{u} < 0$ ) paths. Additionally, elastoplastic elements (components 8 and 9) describe the energy dissipation for small strain amplitudes due to their small yield displacement  $u_y$ , see Fig. 4(f). Finally, Fig. 5 gives a better representation of the comparison of the THM1 system with the experimental results at each level of strain amplitude separately, and clearly shows an almost perfect fit between simulated and recorded curves.

The total number of parameters for the THM1 system is 33 and the identification error is rather small at  $e^2 = 2.50\%$ . Six THM2 components are connected in parallel to describe the shear behaviour of the HDRB experiment, and the identified mathematical parameters are presented in Table 9, along with the corresponding mechanical formulations. Component 1 has softening behavior ( $k_2 < k_1$ ), while the remaining components show hardening behavior ( $k_2 > k_1$ ), see Table 9. Components 1 and 2 have a small yield displacement  $u_y$  and describe energy dissipation for small strain amplitudes, where the rest of the components remain in the elastic range. In Fig. 6, the overall behavior of the THM2 system is compared with experimental data. The comparison shows that the system fails to describe the larger energy dissipation at larger strain amplitudes. The total number of parameters of the THM2 system is 30, and the identification error is  $e^2 = 5.00\%$ , namely twice that of the THM1 system. Additional THM2 components did not help improve the fitting between experimental and simulated curves, meaning that six THM2 is the limit for this case. In closing, more details on the modelling approach for the THM1 can be found in Ref. [9], where the THM1 is solved analytically for the case of the single degree of freedom systems. Ongoing work aims to develop numerical implementation for the case of multi-degree of freedom systems. For the case of THM2, the system can be solved by using Newmark's method combined with Newton-Raphson iterations.

| No. | Component   | $k_0$<br>(kN/mm)     | $k_1$<br>(kN/mm) | $k_2$<br>(kN/mm) | $u_y$<br>(mm)    | $u_{yh}$<br>(mm) |
|-----|---|----------------------|------------------|------------------|------------------|------------------|
| 1   |    | $\gg k_1, k_2^{(1)}$ | 0.283532         | 0.489882         | 0 <sup>(2)</sup> | 64.809           |
| 2   |    | $\gg k_1, k_2^{(1)}$ | 0.000282         | 0.905635         | 0 <sup>(2)</sup> | 136.491          |
| 3   |    | $\gg k_1, k_2^{(1)}$ | 0.000246         | 0.877611         | 0 <sup>(2)</sup> | 108.657          |
| 4   |    | 0.863754             | 0.402485         | -0.792654        | 7.146            | 125.542          |
| 5   |   | 0.157047             | 0.000238         | -0.285050        | 43.938           | 151.692          |
| 6   |  | 0.172839             | 0.000547         | -0.271989        | 18.760           | 80.117           |
| 7   |  | 0.056183             | 0.044945         | -0.006864        | 3.331            | 21.299           |
| 8   |  | 3.225241             | 0 <sup>(3)</sup> | 0 <sup>(3)</sup> | 0.597            | - <sup>(4)</sup> |
| 9   |  | 67.445070            | 0 <sup>(3)</sup> | 0 <sup>(3)</sup> | 0.041            | - <sup>(4)</sup> |
|     |   |                      |                  |                  | $e^2$            | 2.50 %           |

Table 8: Mechanical system using the THM1 model components (33 parameters)

<sup>(1)</sup>A very large value of  $k_0 \gg k_1, k_2$  corresponds to a stiff elastic spring and is neglected.

<sup>(2)</sup>THM1 becomes a trilinear elastic spring for  $u_y = 0$ .

<sup>(3)</sup> THM1 becomes an elastoplastic element for  $k_1 = k_2 = 0$ .

<sup>(4)</sup>Because  $k_1 = k_2 = 0$ ,  $u_{yh}$  does not denote any change of stiffness, it is inconsequential.

## 4 CONCLUSIONS

Two extensions of the well-known BHM are introduced for modelling hardening and softening effects observed in base isolators. More specifically, THM1 exhibits three plastic phases and one elastic phase, while THM2 exhibits three plastic phases and two elastic phases. The change of slope in the plastic phases during unloading ( $ui < 0$ ), does not occur at the

same displacement level for either model. Furthermore, the dissipated energy per cycle of amplitude  $u_a$  decreases in the case of hardening and increases in the case of softening for the THM1 model, while in THM2 model the dissipated energy remains constant. A set of cyclic shear tests on an existing HDRB under a wide range of strain amplitudes shows that the shear behaviour observed can be described by a parallel system, which comprises only one type of component, namely the THM1 with identification error  $e^2 = 2.50\%$ . On the other hand, a parallel-type THM2 model fails in describe the behaviour of the HDRB since it does not account for increasing energy dissipation at larger amplitudes (the identification error here is  $e^2 = 5.00\%$ ). Compared to THM2, THM1 has the following advantages: (a) It accounts for larger energy dissipation at larger strain amplitudes; (b) it better describes the behaviour observed during the loading ( $u\dot{u} > 0$ ) and unloading ( $u\dot{u} < 0$ ) paths in the HDRB; and (c) through a proper choice of parameters, can be reduced to simpler models, namely a trilinear elastic spring and an elastoplastic element.

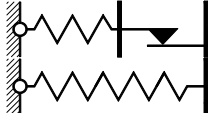
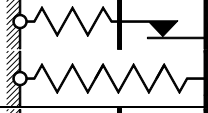
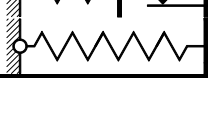
| No. | Component   | $k_0$<br>(kN/mm) | $k_1$<br>(kN/mm) | $k_2$<br>(kN/mm) | $u_y$<br>(mm) | $u_{yh}$<br>(mm) |
|-----|---|------------------|------------------|------------------|---------------|------------------|
| 1   |    | 3.316369         | 0.097634         | 0.066989         | 0.604         | 34.120           |
| 2   |   | 67.826800        | 0.034459         | 0.242161         | 0.041         | 181.563          |
| 3   |  | 0.583996         | 0.082570         | 0.258475         | 7.945         | 102.741          |
| 4   |  | 0.360200         | 0.159367         | 0.287472         | 128.456       | 139.534          |
| 5   |  | 0.315248         | 0.115504         | 0.225922         | 20.728        | 99.702           |
| 6   |  | 0.142166         | 0.010595         | 0.325443         | 43.731        | 162.318          |
|     |   |                  |                  |                  | $e^2$         | 5.00%            |

Table 9: Parallel mechanical system using the THM2 model (30 parameters)

**Acknowledgements** The authors acknowledge the assistance of Profs. G. Oliveto, F.C. Ponzo and G. Serino through project ReLUIIS D.P.C 2014-2016 and Prof. A.G. Sextos through the Horizon 2020 MSCA-RISE-2015 project No. 691213.

## REFERENCES

- [1] A.A. Markou and G.D. Manolis, Mechanical formulations for bilinear and trilinear hysteretic models used in base isolators. *Bulletin of Earthquake Engineering*, **14**, 3591-3611, 2016.

- [2] J. Besson, G. Cailletaud, J.L. Chaboche, S. Forest and M. Bletry, M, *Non-linear mechanics of materials*. Springer-Verlag, Heidelberg, 2010.
- [3] Y.K. Wen, Method for random vibration of hysteretic systems, *Journal Engineering Mechanics ASCE*, **102**, 249-263, 1976.
- [4] G. Oliveto, N.D. Oliveto and A. Athanasiou, Constrained optimization for 1-D dynamic and earthquake response analysis of hybrid base-isolation systems. *Soil Dynamics Earthquake Engineering* **67**, 44-53, 2014.

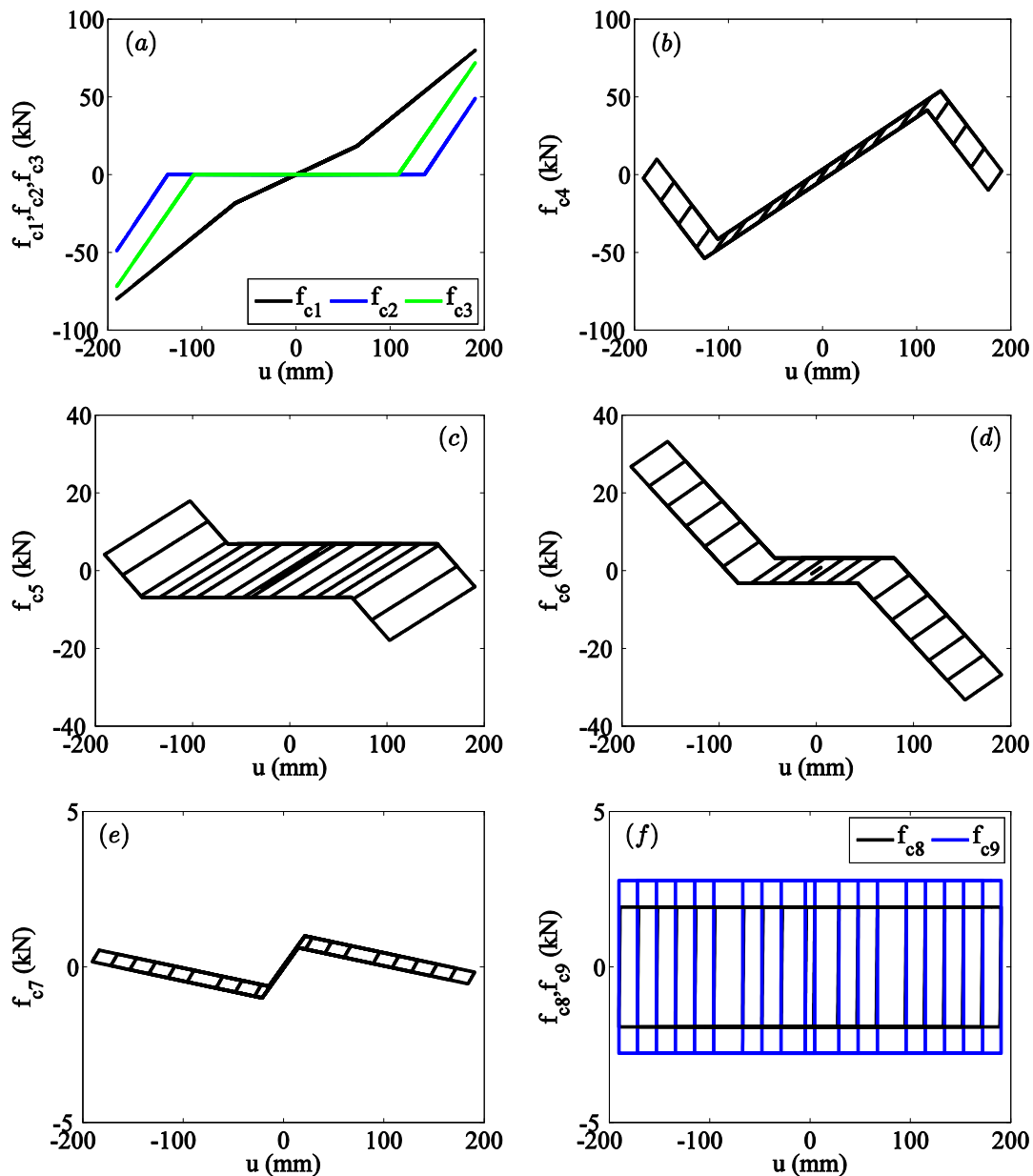


Figure 4: Force-displacement curves of each separate component of the THM1 model

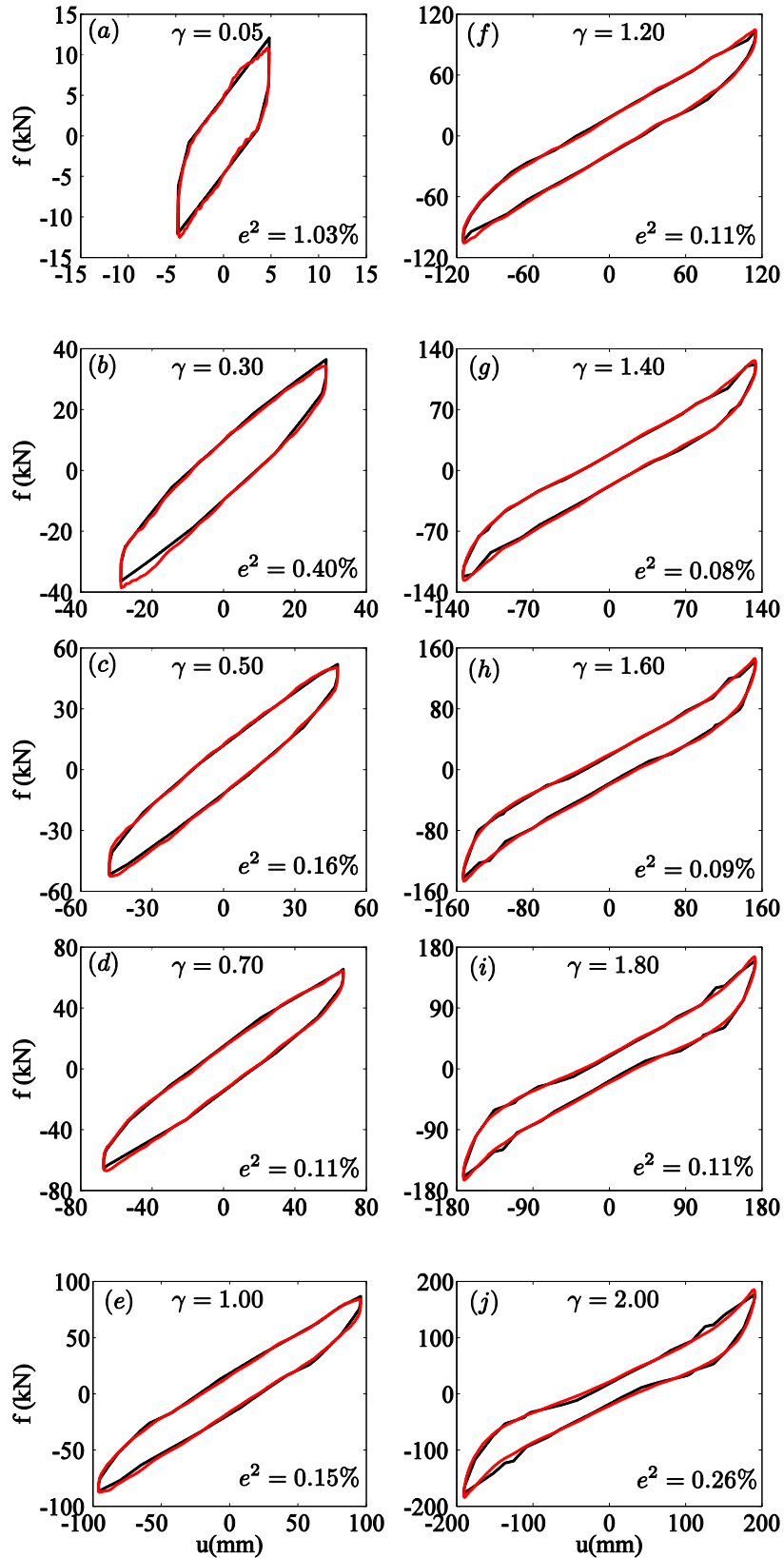


Figure 5: Identification of force-displacement curves of THM1 model using the 3rd cycle of harmonic tests at 10 strain amplitudes, frequency 0.5 Hz, compressive stress 6 MPa (black color: numerical simulations; red color: experimental data)

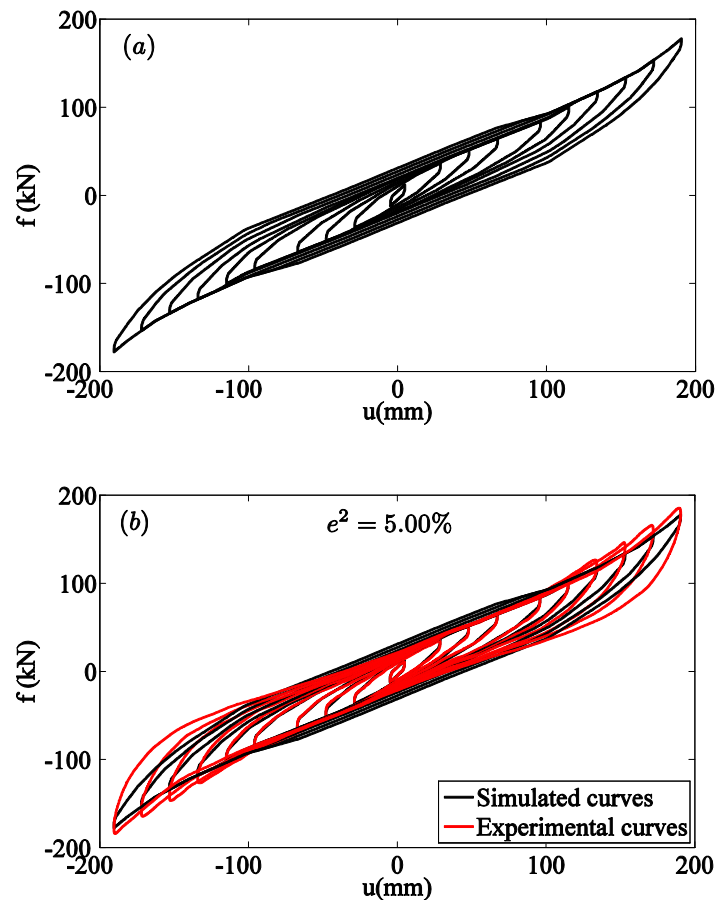


Figure 6: (a) THM2 force-displacement curves; (b) comparisons with experimental data

- [5] P.C. Tsopelas, M.C. Constantinou and A.M. Reinhorn AM (1994) *3D-BASIS-ME: Computer program for Nonlinear Dynamic Analysis of Seismically Isolated Single and Multiple Structures and Liquid Storage Tanks*, Report NCEER-94-0010, University at Buffalo, New York, 1994.
- [6] A.A. Markou, G. Oliveto and A. Athanasiou, Response simulation of hybrid base isolation systems under earthquake excitation, *Soil Dynamics Earthquake Engineering* **84**,120-133, 2016.
- [7] T. Ray, A.A. Sarlis, A.M. Reinhorn and M.C. Constantinou MC, Hysteretic models for sliding bearings with varying frictional force, *Earthquake Engineering Structural Dynamics* **42**, 2341-2360, 2013.
- [8] T. Ray and A.M. Reinhorn, Enhanced smooth hysteretic model with degrading properties varying frictional force, *Journal Structural Engineering ASCE* **140**(1), 2013.
- [9] A. A. Markou, G. Oliveto, A. Mossucca and F.C. Ponzo, *Laboratory experimental tests on elastomeric bearing from the Solarino project. Progetto di Ricerca DPC-RELUIS, Linea di Ricerca 6: Isolamento e Dissipazione, Coordinatori: Ponzo FC and Serino G*, University of Basilicata, Italy, 2014.
- [10] N. Hansen, *The CMA evolution strategy: A (web-based) tutorial*, 2011. (<https://www.lri.fr/~hansen/cmatutorial.pdf>)